Am J Transl Res 2021;13(11):12338-12351
www.ajtr.org /ISSN:1943-8141/AJTR0127738

Original Article

AKIP1 promotes tumor progression by cancer-related pathways and predicts prognosis in tongue squamous cell carcinoma

Ning Wang[1], Dan Bai[2], Einar Kristiansen[3], Ruoyu Deng[4], Shijun Zhang[1]

[1]*Department of Orthopaedics, Qilu Hospital of Shandong University, Jinan 250012, Shandong, China;* [2]*Department of Hematology, Qilu Hospital of Shandong University, Jinan 250012, Shandong, China;* [3]*Department of Tumor Biology, Institute of Cancer Research, The Norwegian Radium Hospital, Oslo University Hospital, Oslo 0424, Norway;* [4]*Department of Biostatistics, Shanghai QeeJen Institution, Shanghai 200433, China*

Received December 7, 2020; Accepted August 24, 2021; Epub November 15, 2021; Published November 30, 2021

Abstract: The current study was designed to explore the effect of A-kinase-interacting protein 1 (AKIP1) on tongue squamous cell carcinoma (TSCC) viability and mobility and to investigate its molecular mechanism. Control overexpression (OE-NC group) and AKIP1 overexpression (OE-AKIP1 group) plasmids were transfected into CAL-27 cells; control knockdown (KD-NC group) and AKIP1 knockdown (KD-AKIP1 group) plasmids were transfected into SCC-9 cells. Cellular viability and mobility were determined, and mRNA sequencing was performed followed by RT-qPCR validation. Immunohistochemistry was utilized to detect AKIP1 expression in tumor and adjacent tissues from 90 TSCC patients. AKIP1 was more highly expressed in human TSCC cell lines compared to human normal lingual epithelial cells. Cell proliferation, migration, and invasion were increased in the OE-AKIP1 group compared to the OE-NC group but decreased in the KD-AKIP1 group compared to the KD-NC group. mRNA sequencing revealed 436 differentially expressed genes; most of the genes were mainly enriched in the mTOR, PI3K-Akt, MAPK, Hippo, and Wnt signaling pathways. These findings were subsequently confirmed by RT-qPCR quantification. In TSCC patients, AKIP1 expression was increased in tumor tissues and related to increased tumor size, lymph node metastasis and poor overall survival. AKIP1 is a therapeutic target that regulates multiple tumor-related pathways in TSCC.

Keywords: AKIP1, tongue squamous cell carcinoma, cellular function, mRNA sequencing, pathways

Introduction

Oral cancer is considered the most frequent solid cancer worldwide with an estimated 354,000 new cases and 177,000 deaths occurring each year, accounting for 2.0% of newly diagnosed cases and 1.9% of cancer-related deaths [1, 2]. Tongue squamous cell carcinoma (TSCC) is characterized by malfunctions of mastication, speech, and deglutition and exhibits a marked biologic propensity for aggressive progression with lymph node and/or distant metastases that are eventually related to unfavorable prognosis [3, 4]. Of note, TSCC patients who are diagnosed at an early stage have a favorable prognosis, whereas most patients present with local invasion as well as cervical lymph node metastasis when diagnosed (approximately 40% of all TSCC cases) due to its progression from a premalignant condition to an invasive cancer lacking specific symptoms. Unfortunately, even with combined treatment involving surgery, radiation, and chemotherapy, patient survival remains unsatisfactory [5-8]. Thus, we investigated the mechanisms underlying TSCC to explore novel and potential therapeutic targets of TSCC.

Kinase-interacting protein 1 (AKIP1) is a 23-kDa protein originally identified in breast cancer and prostate cancer [9, 10]. Existing data indicate that AKIP1 is aberrantly expressed and exerts promotive effects on malignant progression in several cancers (such as enhancing cell growth in gastric cancer [11], facilitating cell migration in cervical cancer (CC) [12], and promoting breast cancer cell motility and invasion [13]). In addition, AKIP1 has also been reported to be overexpressed and related to worse prognosis in multiple carcinomas (including colorectal cancer (CRC) [10], breast cancer [13], and gastric cancer [14]).

Considering the oncogenic impact of AKIP1 in tumor progression as well as its relationship with poor prognosis in several cancers, we hypothesized that AKIP1 might function as a tumor promoter in TSCC; however, little is known about AKIP1. In the present study, the purpose was to assess the influence of AKIP1 on cell proliferation, migration, and invasion and its molecular mechanism in TSCC.

Methods

Cell culture

Human TSCC cells HSC-3 (JCRB, Japan), HSC-4 (JCRB, Japan), SCC-4 (ATCC, USA), SCC-9 (ATCC, USA), and CAL-27 (ATCC, USA) were purchased and cultured according to the instructions of suppliers. Normal human oral keratinocytes (NHOKs) (ScienCell, USA) were also purchased and cultured according to the instructions of the supplier. AKIP1 expression in TSCC and NHOK (served as a control) was assessed using reverse transcription-quantitative polymerase chain reaction (RT-qPCR) and western blot.

Transfection

AKIP1 overexpression (OE) plasmid and negative control (NC) overexpression plasmid [constructed with pEX-2 vector (Genepharma, China)] were transfected into CAL-27 cells by Lipofectamine™ 3000 Transfection Reagent (Invitrogen, USA) following instructions of the manufacturer, and the resulting cells are referred to as AKIP1-OE and NC-OE cells, respectively. The AKIP1 knockdown (KD) plasmid and NC-KD plasmid [constructed with pGPH1 (GenePharma, China)] were transfected into SCC-9 cells using the same reagent mentioned above, and the resulting cells are referred to as AKIP1-KD cells and NC-KD cells, respectively. Non-transfected CAL-27 cells and SCC-9 cells served as controls. AKIP1 expression was detected by RT-qPCR and western blot. Cell proliferation (0, 24, 48 and 72 h after transfection), cell apoptosis (48 h after transfection), and cell migration and invasion (24 h after transfection) were detected.

Assessment of viability and mobility

Cell proliferation was measured (CCK-8 assay) using the Cell Counting Kit-8 (Dojindo, Japan). Cell apoptosis was evaluated (Annexin V/propidium iodide (AV/PI)) with the Annexin V-FITC Apoptosis Detection Kit (Sigma, USA). Both assays were performed following the kits' instructions. Cell migration (wound healing assay) and invasion (Transwell assay) were assessed by methods described in previous studies [15, 16].

RNA sequencing (RNA-seq) and bioinformatics analysis

Total RNA was extracted 24 h after transfections using TRIzol® Reagent (Invitrogen, USA) and then subjected to RNA-seq according to the previously mentioned method [17]. Principal component analysis (PCA), volcano plots, cross-analysis with Venn diagrams, Gene Ontology (GO) and Kyoto Encyclopedia of Genes and Genomes (KEGG) were performed according to the previously mentioned methods [18-20].

Screening DEGs and pathways

Cross analysis was used to identify accordant DEGs. Accordant DEGs were defined as the DEGs that met any of following conditions: (1) DEGs were upregulated in the OE term (AKIP1-OE vs. NC-OE) and downregulated in the KD term (AKIP1-KD vs. NC-KD); (2) DEGs were downregulated in the OE term and upregulated in the KD term. The top 50 DEGs were identified according to the rank of the mean absolute value of Log_2FC, which was calculated based on the average of OE absolute log_2FC and KD absolute log_2FC. Potential pathways were initially identified by KEGG enrichment analysis with corresponding DEGs. Subsequently, the top 5 signaling pathways (mammalian target of rapamycin (mTOR), phosphatidylinositol-3-hydroxykinase/threonine kinase (PI3K-Akt), mitogen-activated protein kinase (MAPK) signaling pathway, Hippo, and Wnt signaling pathways) frequently associated with TSCC were further screened from potential pathways related to TSCC progression according to existing data [21-25]. Moreover, the expression of the DEGs implicated in the 5 selected signaling pathways was further validated by RT-qPCR.

RT-qPCR

RNA was reverse transcribed to cDNA by PrimeScript™ RT Master Mix (Takara, Japan). TB Green™ Fast qPCR Mix (Takara, Japan) was used for qPCR. GAPDH was selected as an internal reference. The primers used were in Supplementary Table 1. The $2^{-\Delta\Delta Ct}$ method was utilized to calculate the relative mRNA expression.

Western blotting

After using RIPA buffer (Sigma, USA) for the extraction of total protein, the protein concentration was measured (Bicinchoninic Acid Kit for Protein Determination (Sigma, USA)). Subsequently, the protein sample was separated with NuPAGE Bis-Tris Gels 4-12% (Thermo, USA) and transferred to a polyvinylidene fluoride membrane (PALL, USA). After blocking with 5% skim milk for 2 h, the membrane was incubated with the primary antibody (AKIP1 polyclonal antibody (dilution 1:1000, Invitrogen, USA) and GAPDH polyclonal antibody (1:2000, Invitrogen, USA)) overnight at 4°C followed by incubation with the secondary antibody (goat anti-rabbit IgG (H+L) poly-HRP (dilution 1:10000, Invitrogen, USA)) for 1 h at room temperature. Blots were visualized by chemiluminescence using the Pierce™ECL Plus western blotting Substrate (Thermo, USA) followed by exposure to X-ray film (Kodak, USA). GAPDH served as the internal reference.

TSCC patients and specimens

Tumor and adjacent tissues were obtained from 90 TSCC patients who underwent surgical resection at our hospital between Jan 2015 and Dec 2019. The screening criteria inclusion in the study were as follows: (1) pathologically diagnosed with TSCC; (2) age ≥18 years; (3) underwent resection without other treatments for tumors before surgery; (4) TSCC tissue and paired adjacent tissue removed by surgery were accessible and available for immunohistochemical (IHC) staining; and (5) clinical data and survival data were complete. Patient medicine information (clinical data and survival data) was collected from the computer-based patient record systems of our hospital. In addition, overall survival (OS) was calculated as the date of surgical resection to the date of death or last follow-up. This study was approved by the Ethics Committee of our hospital, and written informed consent was collected from the patients or their family members.

AKIP1 detection by IHC staining

IHC staining was utilized to assess AKIP1 expression in TSCC tissue specimens and paired adjacent tissue specimens. In brief, IHC staining was performed as follows: formalin-fixed paraffin-embedded tissue specimens were cut into 4-μm sections followed by deparaffination in xylene (Sigma, USA) (3 times) and rehydration in an ethanol gradient (100%, 95%, 70%, and 50%) (Sigma, USA). Nonspecific peroxidase activity was blocked with H_2O_2 (Sigma, USA), and antigen retrieval was performed using citrate buffer. The sample was incubated with the primary antibody [AKIP1 Polyclonal Antibody (rabbit anti-AKIP1, dilution 1:30, Invitrogen, USA)] overnight at 4°C. Next, incubation was performed with secondary antibody [goat anti-rabbit IgG (H+L) secondary antibody (dilution 1:500, Invitrogen, USA)] for 30 min. Then, sections were treated with diaminobenzidine (DAKO, USA), counterstained with hematoxylin (Sigma, USA), viewed under a microscope and photographed (a Nikon ECLIPSE E600 microscope (Nikon Instruments, USA)). AKIP1 expression was assessed [1].

Statistical analysis

SPSS 22.0 statistical software (IBM, Chicago, Illinois, USA) was used for data analysis, and GraphPad Prism 7.02 (GraphPad Software Inc., San Diego, California, USA) was adopted for graph plotting. Experimental data are expressed as the mean with standard deviation (SD). The comparison between groups was determined using one-way ANOVA followed by Dunnett's multiple comparisons test. Comparisons between two groups was determined using unpaired t tests. Clinical data of TSCC patients were described as the mean with SD or number with percentage (No. (%)). McNemar's test was utilized for comparison of AKIP1 expression between tumor tissue and adjacent tissue. The chi-square test or Spearman's rank correlation test was utilized for correlation analysis. OS was displayed using Kaplan-Meier curves, and the comparison of OS between two groups was determined using the log-rank test. Univariate and multivariate Cox proportional hazards regression model

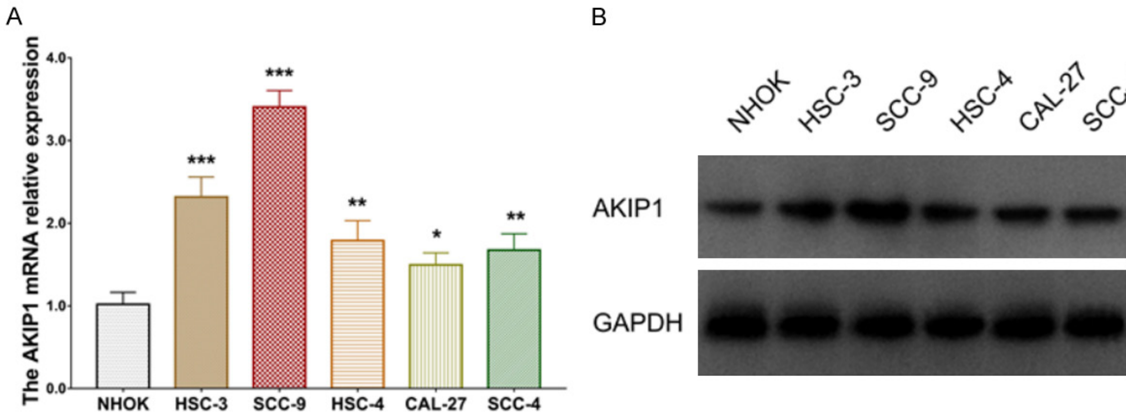

Figure 1. AKIP1 expression. AKIP1 mRNA (A) and protein (B) expression.

analyses were utilized to analyze OS-related factors. Statistical significance was set at *P* <0.05. In addition, *P* values <0.05, <0.01, and <0.001 in the experimental figures are marked as *, **, and ***, respectively; a nonsignificant difference is denoted as NS.

Results

AKIP1 expression

AKIP1 mRNA (**Figure 1A**) and protein (**Figure 1B**) expression was greater in human TSCC cell lines (HSC-3 (*P*<0.001), SCC-9 (*P*<0.001), HSC-4 (*P*<0.01), CAL-27 (*P*<0.05) and SCC-4 (*P*<0.05)) compared with NHOK cells. Subsequently, further experiments were performed in SCC-9 cells and CAL-27 cells.

AKIP1 expression after transfection

In CAL-27 cells, AKIP1 mRNA (*P*<0.001) (**Figure 2A**) and protein (**Figure 2B**) expression was enhanced in the AKIP1-OE group compared to the NC-OE group. In contrast, in SCC-9 cells, AKIP1 mRNA (*P*<0.001) (**Figure 2C**) and protein (**Figure 2D**) expression was lower in the AKIP1-KD group than in the NC-KD group. These findings indicated successful transfection.

Effect of AKIP1 on cell proliferation and apoptosis

CAL-27 cell proliferation was elevated at 48 h (*P*<0.05) and 72 h (*P*<0.05) in the AKIP1-OE group compared to the NC-OE group (**Figure 3A**), whereas CAL-27 cell apoptosis was inhibited at 48 h (*P*<0.05) in the AKIP1-OE group compared to the NC-OE group (**Figure 3B**, **3C**). SCC-9 cell proliferation was reduced at 48 h (*P*<0.05) and 72 h (*P*<0.01) in the AKIP1-KD group compared to the NC-KD group (**Figure 3D**), whereas SCC-9 apoptosis was enhanced at 48 h (*P*<0.01) in the AKIP1-KD group compared to the NC-KD group (**Figure 3E**, **3F**).

AKIP's effects on cell migration and invasion

The CAL-27 cell migration rate (*P*<0.05) (**Figure 4A**, **4B**) and number of invasive cells (*P*<0.05) (**Figure 4C**, **4D**) were increased in the AKIP1-OE group compared to the NC-OE group. The SCC-9 cell migration rate (*P*<0.05) (**Figure 4E**, **4F**) and invasive cell number (*P*<0.01) (**Figure 4G**, **4H**) were decreased in the AKIP1-KD group compared to the NC-KD group.

PCA plots and heatmap analysis of the mRNA expression profile after AKIP1 modification

To explore the comprehensive molecular mechanism of AKIP1 in TSCC pathogenesis, we performed RNA sequencing and bioinformatics in NC-OE, AKIP1-OE, NC-KD, and AKIP1-KD cells. PCA plot (**Figure 5A**) and heatmap analyses (**Figure 5B**) of the mRNA expression profile revealed separation of the AKIP1-OE group from the NC-OE group as well as the AKIP1-KD group from the NC-KD group.

Volcano plot, GO enrichment, and KEGG enrichment analyses for DEGs induced by AKIP1 modification

In CAL-27 cells, a volcano plot revealed 593 upregulated DEGs and 607 downregulated

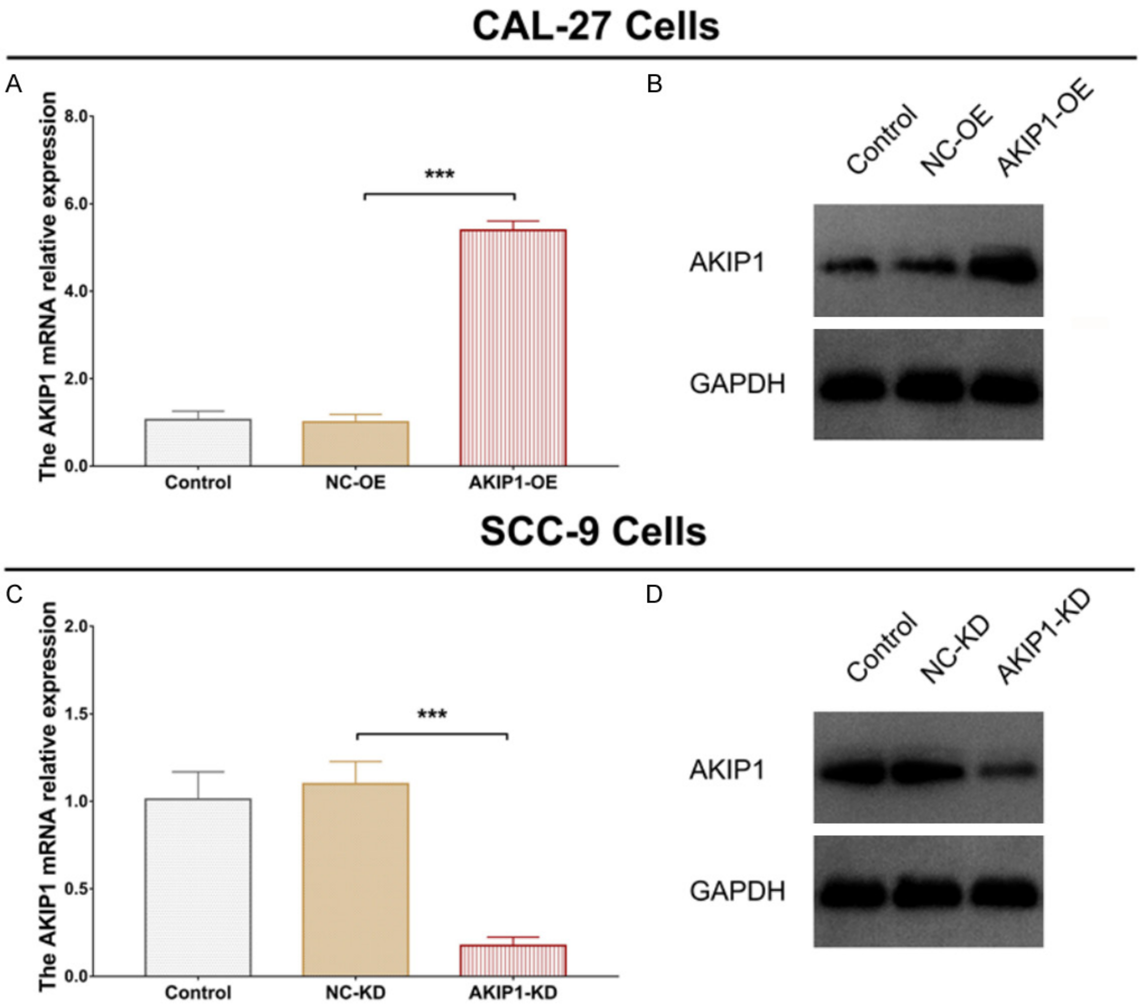

Figure 2. AKIP1 expression after transfection. AKIP1 mRNA (A) and protein (B) expression after transfection in CAL-27 cells; AKIP1 mRNA (C) and protein (D) expression after transfection in SCC-9 cells.

DEGs in the AKIP1-OE group vs. the NC-OE group (**Figure 6A**). GO enrichment analysis revealed that DEGs in the AKIP1-OE group vs. NC-OE group were enriched in various biolog processes (e.g., positive regulation of cell proliferation and transcription), cellular components (e.g., nucleus and cytosol) and molecular functions (e.g., ATP and RNA binding) (**Figure 6B**). KEGG enrichment analysis revealed that DEGs in the AKIP1-OE group vs. the NC-OE group were mainly enriched in the PI3K-Akt, MAPK, mTOR, and chemokine signaling pathways as well as axon guidance (**Figure 6C**).

In SCC-9 cells, a volcano plot revealed 790 upregulated DEGs and 894 downregulated DEGs in the AKIP1-KD group vs. the NC-KD group (**Figure 6D**). GO enrichment analysis illustrated that DEGs in the AKIP1-KD group vs. NC-KD group were concentrated in various biologic processes (e.g., positive regulation of transcription and apoptosis), cellular components (e.g., cytoplasm and nucleoplasm) and molecular functions (e.g., RNA and receptor binding) (**Figure 6E**). KEGG enrichment analysis displayed that DEGs in the AKIP1-KD group vs. NC-KD group were obviously concentrated in PI3K-Akt, MAPK, mTOR, oxytocin signaling pathways, and endocytosis (**Figure 6F**).

Venn diagram, GO enrichment, and KEGG enrichment analyses for accordant DEGs induced by AKIP1 modification

Venn diagram analysis displayed the overlapping patterns of DEGs in the AKIP1-OE group

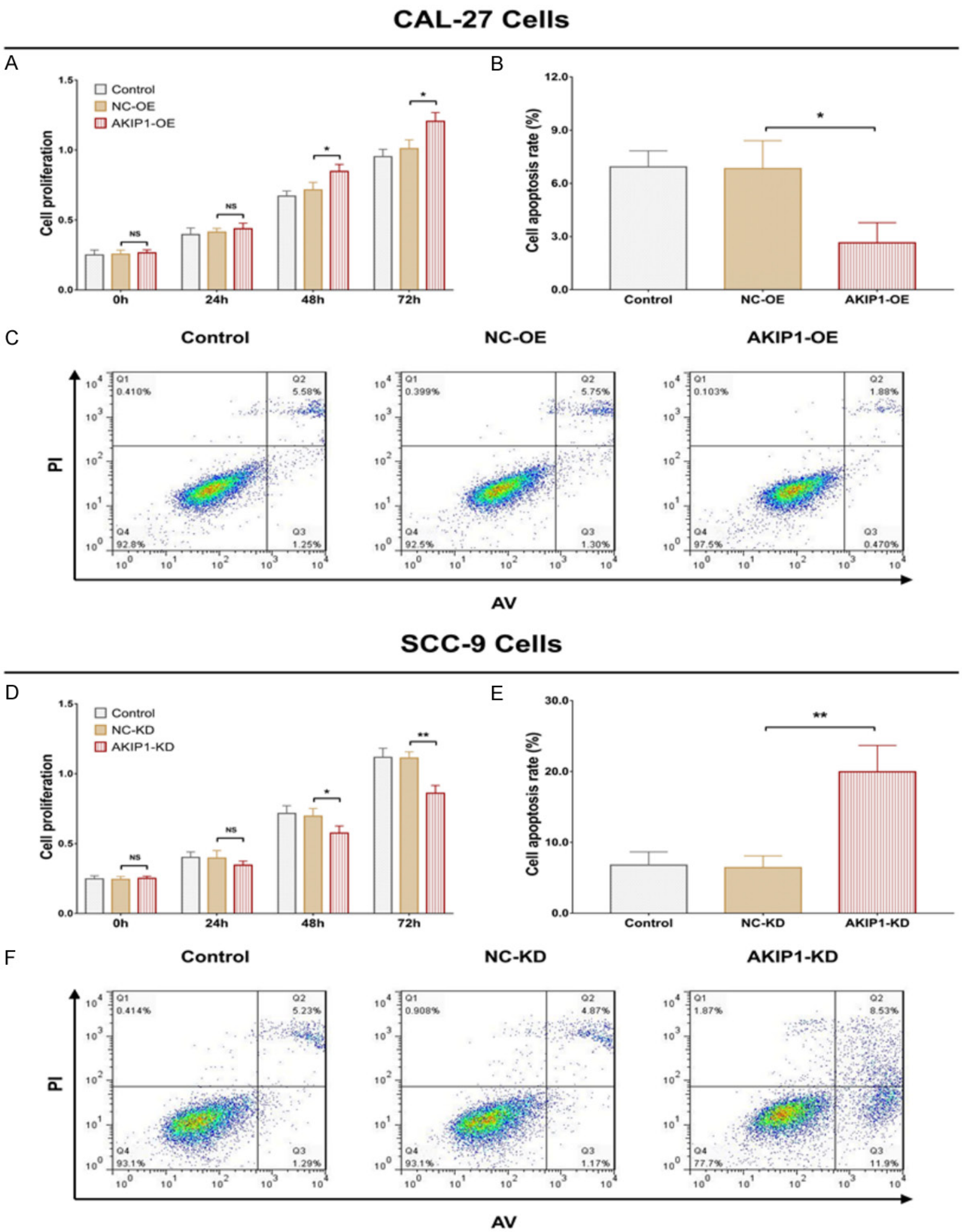

Figure 3. Cell proliferation and apoptosis. The effect of AKIP1 overexpression on promoting cell proliferation (A) and repressing apoptosis (B, C) in CAL-27 cells. The effect of AKIP1 knockdown on inhibiting cell proliferation (D) and facilitating apoptosis (E, F) in SCC-9 cells.

vs. NC-OE group and the AKIP1-KD group vs. NC-KD group. A total of 436 accordant DEGs were identified, including 240 DEGs upregulated in the AKIP1-OE group vs. NC-OE group and downregulated in the AKIP1-KD group vs. NC-KD group as well as 196 DEGs downregu-

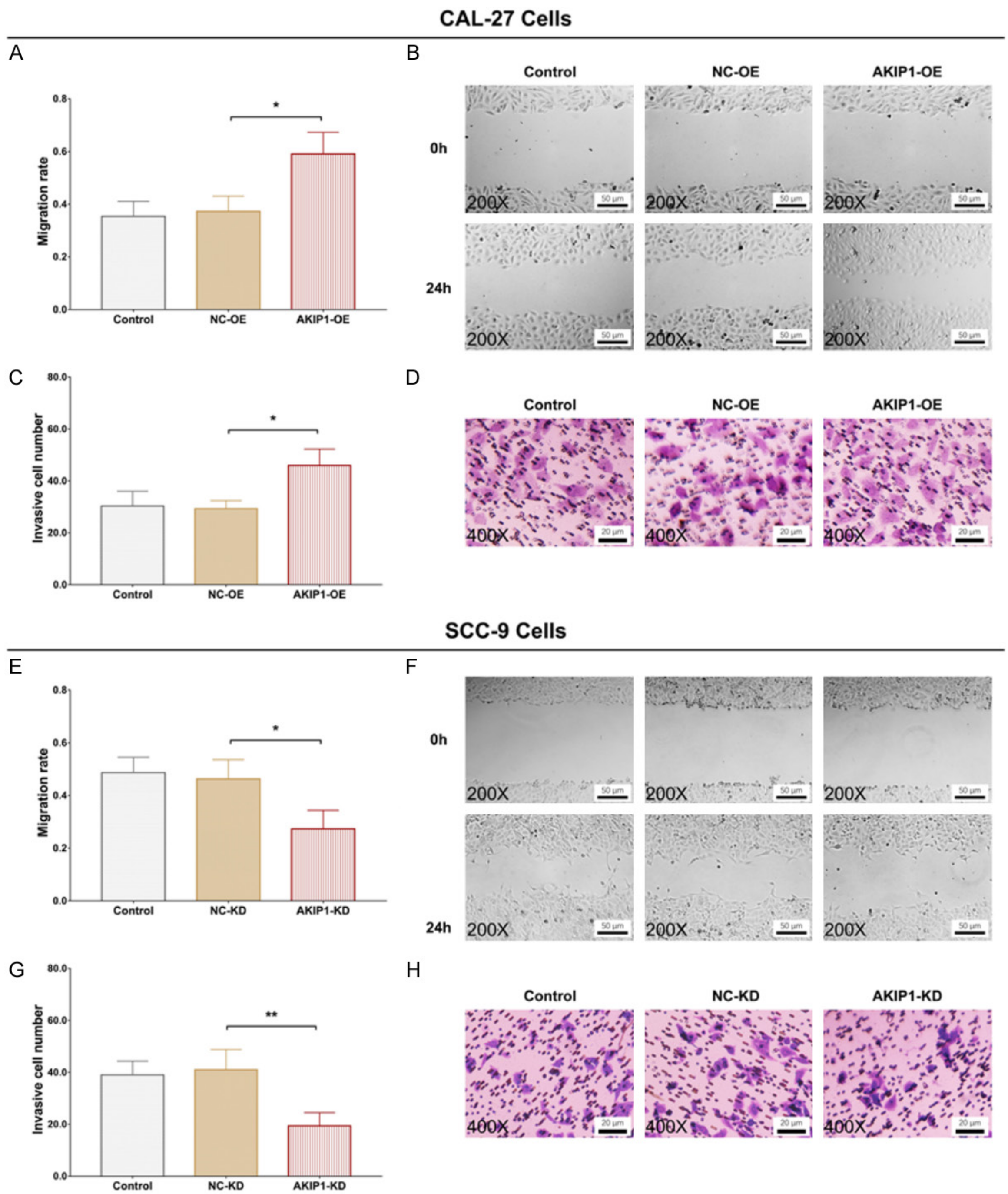

Figure 4. Cell migration and invasion. The effect of AKIP1 overexpression on accelerating cell migration (A, B) and increasing invasion (C, D) in CAL-27 cells; the effect of AKIP1 knockdown on suppressing cell migration (E, F) and decreasing invasion (G, H) in SCC-9 cells.

lated in the AKIP1-OE group vs. NC-OE group and upregulated in the AKIP1-KD group vs. NC-KD group (**Figure 7A**). In addition, the top 50 DEGs detected by RNA sequencing are listed in Supplementary Table 2 for easy reference.

GO enrichment analysis illustrated that accordant DEGs were concentrated in various biologic processes (e.g., Wnt signaling pathway and positive regulation of cell proliferation), cellular components (e.g., cytosol and extracellular exosome) and molecular functions

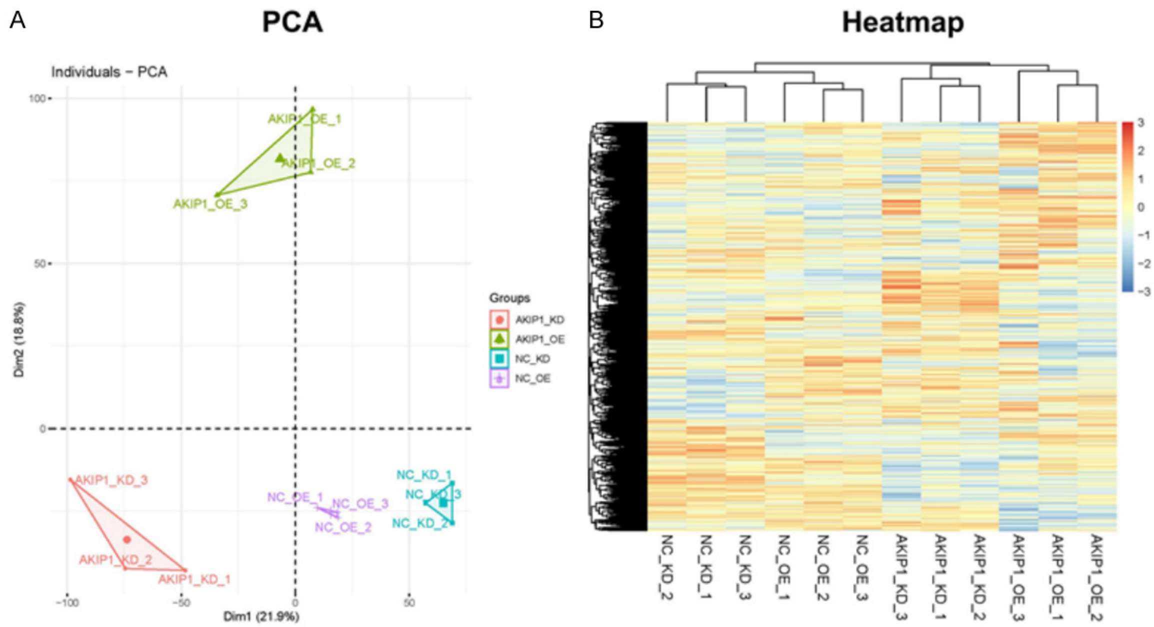

Figure 5. PCA plots and heatmap analysis. PCA plot (A) and heatmap analyses (B) of the mRNA expression profile after AKIP1 modification.

(e.g., protein and ATP binding) (**Figure 7B**). Importantly, KEGG enrichment analysis showed that accordant DEGs were concentrated in mTOR, PI3K-Akt, MAPK, Hippo, and Wnt signaling pathways (**Figure 7C**).

Validation for 5 key cancer-related pathways

According to KEGG enrichment analysis of the accordant DEGs, possible pathways were initially identified. Among these pathways, 5 signaling pathways frequently associated with TSCC (including mTOR, PI3K-Akt, MAPK, Hippo, and Wnt signaling pathways) were further identified (Supplementary Table 3). Hence, we further validated the relative expression of these accordant DEGs that were implicated in these 5 cancer-related pathways by RT-qPCR. The data showed that AKIP1 overexpression activated the mTOR (Supplementary Figure 1A), PI3K-Akt (Supplementary Figure 1B), MAPK (Supplementary Figure 1C), Hippo (Supplementary Figure 1D) and Wnt signaling pathways (Supplementary Figure 1E) in CAL-27 cells. Moreover, AKIP1 knockdown inactivated the mTOR (Supplementary Figure 1F), PI3K-Akt (Supplementary Figure 1G), MAPK (Supplementary Figure 1H), Hippo (Supplementary Figure 1I) and Wnt signaling pathways (Supplementary Figure 1J) in SCC-9 cells. In summary, these data suggest that the impact of AKIP1 on TSCC cell malignant behavior might be related to its effect on activating the mTOR, PI3K-Akt, MAPK, Hippo, and Wnt signaling pathways.

Association of AKIP1 with clinical features and OS

IHC examples of TSCC patients with AKIP1 high/low expression in the tumor or adjacent tissue are presented (**Figure 8A**). AKIP1 expression was increased in tumor tissue compared to adjacent tissue ($P<0.001$) (**Table 1**). Regarding clinical features, high expression of tumor AKIP1 was correlated with higher T stage ($P=0.003$), N stage ($P=0.022$) and TNM stage ($P<0.001$) (**Table 2**). In addition, high tumor AKIP1 expression was correlated with poor OS in TSCC patients ($P=0.027$) (**Figure 8B**). Furthermore, high tumor AKIP1 expression (P=0.039) and TNM stage (III/IV vs. II/I) ($P<0.001$) were related to worse OS. High tumor AKIP1 expression ($P=0.119$) was not an independent factor predicting OS, whereas pathological grade (G3 vs. G1/2) ($P=0.048$) and TNM stage (III/IV vs. II/I) ($P=0.001$) independently predicted worse OS (**Table 3**).

Discussion

AKIP1 is involved in the pathogenesis of several cancers. For instance, one previous study

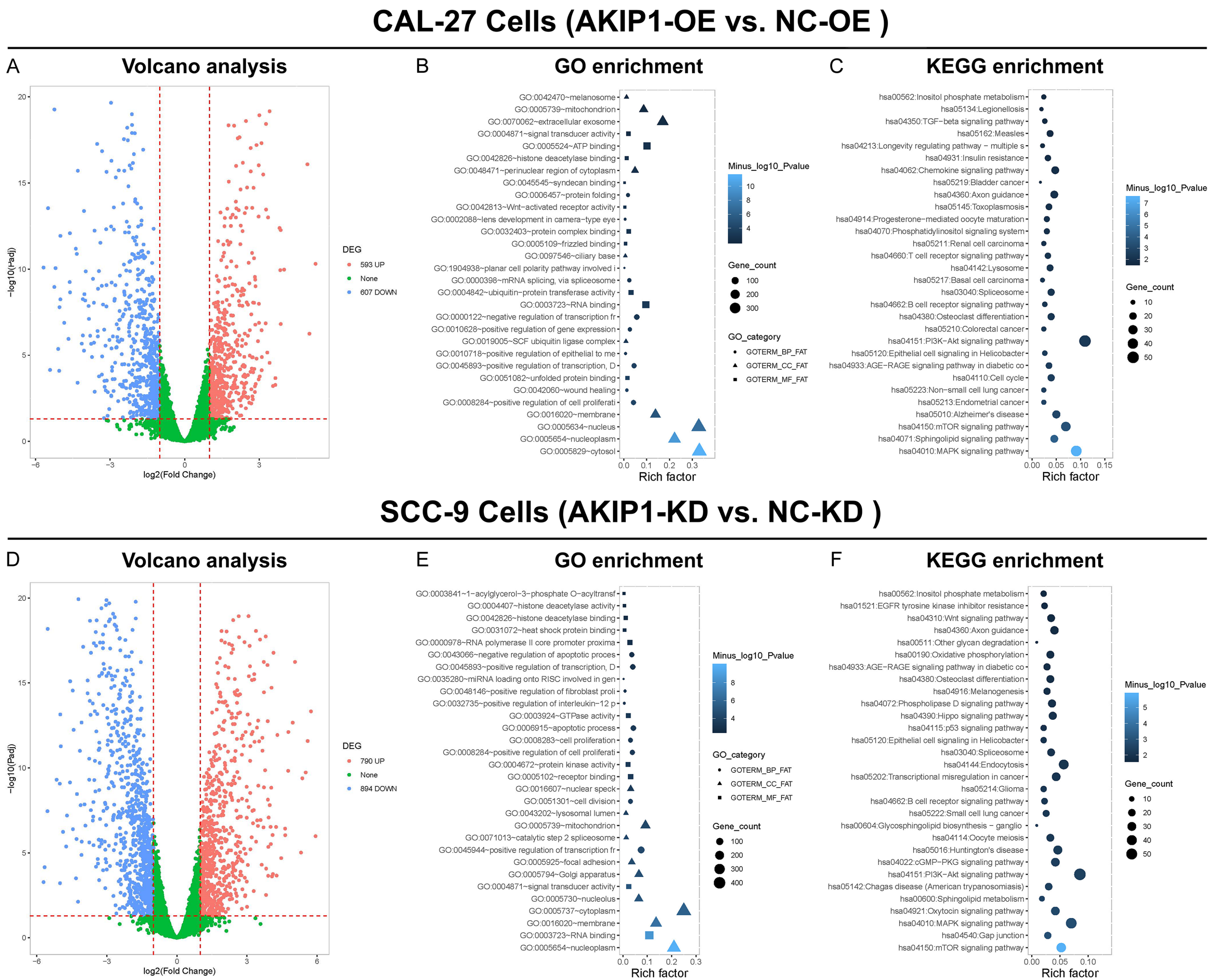

CAL-27 Cells (AKIP1-OE vs. NC-OE)
A
Volcano analysis
−log10(Padj)
log2(Fold Change)
DEG
593 UP
None
607 DOWN
B
GO enrichment
GO:0042470~melanosome
GO:0005739~mitochondrion
GO:0070062~extracellular exosome
GO:0004871~signal transducer activity
GO:0005524~ATP binding
GO:0042826~histone deacetylase binding
GO:0048471~perinuclear region of cytoplasm
GO:0045545~syndecan binding
GO:0006457~protein folding
GO:0042813~Wnt-activated receptor activity
GO:0002088~lens development in camera-type eye
GO:0032403~protein complex binding
GO:0005109~frizzled binding
GO:0097546~ciliary base
GO:1904938~planar cell polarity pathway involved i
GO:0000398~mRNA splicing, via spliceosome
GO:0004842~ubiquitin-protein transferase activity
GO:0003723~RNA binding
GO:0000122~negative regulation of transcription fr
GO:0010628~positive regulation of gene expression
GO:0019005~SCF ubiquitin ligase complex
GO:0010718~positive regulation of epithelial to me
GO:0045893~positive regulation of transcription, D
GO:0051082~unfolded protein binding
GO:0042060~wound healing
GO:0008284~positive regulation of cell proliferati
GO:0016020~membrane
GO:0005634~nucleus
GO:0005654~nucleoplasm
GO:0005829~cytosol
Rich factor
Minus_log10_Pvalue
Gene_count
GO_category
GOTERM_BP_FAT
GOTERM_CC_FAT
GOTERM_MF_FAT
C
KEGG enrichment
hsa00562:Inositol phosphate metabolism
hsa05134:Legionellosis
hsa04350:TGF−beta signaling pathway
hsa05162:Measles
hsa04213:Longevity regulating pathway − multiple s
hsa04931:Insulin resistance
hsa04062:Chemokine signaling pathway
hsa05219:Bladder cancer
hsa04360:Axon guidance
hsa05145:Toxoplasmosis
hsa04914:Progesterone−mediated oocyte maturation
hsa04070:Phosphatidylinositol signaling system
hsa05211:Renal cell carcinoma
hsa04660:T cell receptor signaling pathway
hsa04142:Lysosome
hsa05217:Basal cell carcinoma
hsa03040:Spliceosome
hsa04662:B cell receptor signaling pathway
hsa04380:Osteoclast differentiation
hsa05210:Colorectal cancer
hsa04151:PI3K−Akt signaling pathway
hsa05120:Epithelial cell signaling in Helicobacter
hsa04933:AGE−RAGE signaling pathway in diabetic co
hsa04110:Cell cycle
hsa05223:Non−small cell lung cancer
hsa05213:Endometrial cancer
hsa05010:Alzheimer's disease
hsa04150:mTOR signaling pathway
hsa04071:Sphingolipid signaling pathway
hsa04010:MAPK signaling pathway
Rich factor
Minus_log10_Pvalue
Gene_count
SCC-9 Cells (AKIP1-KD vs. NC-KD)
D
Volcano analysis
−log10(Padj)
log2(Fold Change)
DEG
790 UP
None
894 DOWN
E
GO enrichment
GO:0003841~1−acylglycerol−3−phosphate O−acyltransf
GO:0004407~histone deacetylase activity
GO:0042826~histone deacetylase binding
GO:0031072~heat shock protein binding
GO:0000978~RNA polymerase II core promoter proxima
GO:0043066~negative regulation of apoptotic proces
GO:0045893~positive regulation of transcription, D
GO:0035280~miRNA loading onto RISC involved in gen
GO:0048146~positive regulation of fibroblast proli
GO:0032735~positive regulation of interleukin−12 p
GO:0003924~GTPase activity
GO:0006915~apoptotic process
GO:0008283~cell proliferation
GO:0008284~positive regulation of cell proliferati
GO:0004672~protein kinase activity
GO:0005102~receptor binding
GO:0016607~nuclear speck
GO:0051301~cell division
GO:0043202~lysosomal lumen
GO:0005739~mitochondrion
GO:0071013~catalytic step 2 spliceosome
GO:0045944~positive regulation of transcription fr
GO:0005925~focal adhesion
GO:0005794~Golgi apparatus
GO:0004871~signal transducer activity
GO:0005730~nucleolus
GO:0005737~cytoplasm
GO:0016020~membrane
GO:0003723~RNA binding
GO:0005654~nucleoplasm
Rich factor
Minus_log10_Pvalue
GO_category
GOTERM_BP_FAT
GOTERM_CC_FAT
GOTERM_MF_FAT
Gene_count
F
KEGG enrichment
hsa00562:Inositol phosphate metabolism
hsa01521:EGFR tyrosine kinase inhibitor resistance
hsa04310:Wnt signaling pathway
hsa04360:Axon guidance
hsa00511:Other glycan degradation
hsa00190:Oxidative phosphorylation
hsa04933:AGE−RAGE signaling pathway in diabetic co
hsa04380:Osteoclast differentiation
hsa04916:Melanogenesis
hsa04072:Phospholipase D signaling pathway
hsa04390:Hippo signaling pathway
hsa04115:p53 signaling pathway
hsa05120:Epithelial cell signaling in Helicobacter
hsa03040:Spliceosome
hsa04144:Endocytosis
hsa05202:Transcriptional misregulation in cancer
hsa05214:Glioma
hsa04662:B cell receptor signaling pathway
hsa05222:Small cell lung cancer
hsa00604:Glycosphingolipid biosynthesis − ganglio
hsa04114:Oocyte meiosis
hsa05016:Huntington's disease
hsa04022:cGMP−PKG signaling pathway
hsa04151:PI3K−Akt signaling pathway
hsa05142:Chagas disease (American trypanosomiasis)
hsa00600:Sphingolipid metabolism
hsa04921:Oxytocin signaling pathway
hsa04010:MAPK signaling pathway
hsa04540:Gap junction
hsa04150:mTOR signaling pathway
Rich factor
Minus_log10_Pvalue
Gene_count

Figure 6. Volcano plot and enrichment analyses. Volcano plot (A), GO enrichment analyses (B) and KEGG enrichment analyses (C) for DEGs in the AKIP1-OE group vs. NC-OE group of CAL-27 cells; Volcano plot (D), GO enrichment analyses (E) and KEGG enrichment analyses (F) for DEGs in the AKIP1-KD group vs. NC-KD group of SCC-9 cells.

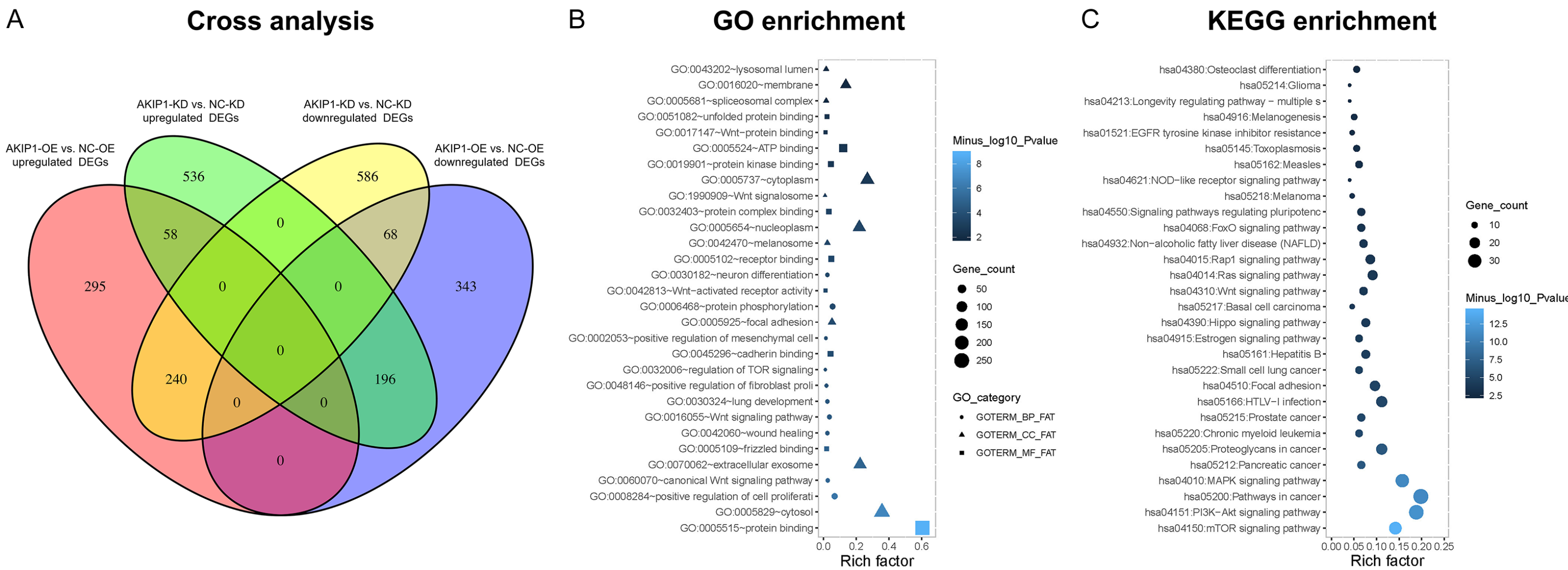

Figure 7. Venn diagram analysis and enrichment analyses for accordant DEGs. Venn diagram analysis (A), GO enrichment analyses (B) and KEGG enrichment analyses (C) for DEGs induced by AKIP1 modification.

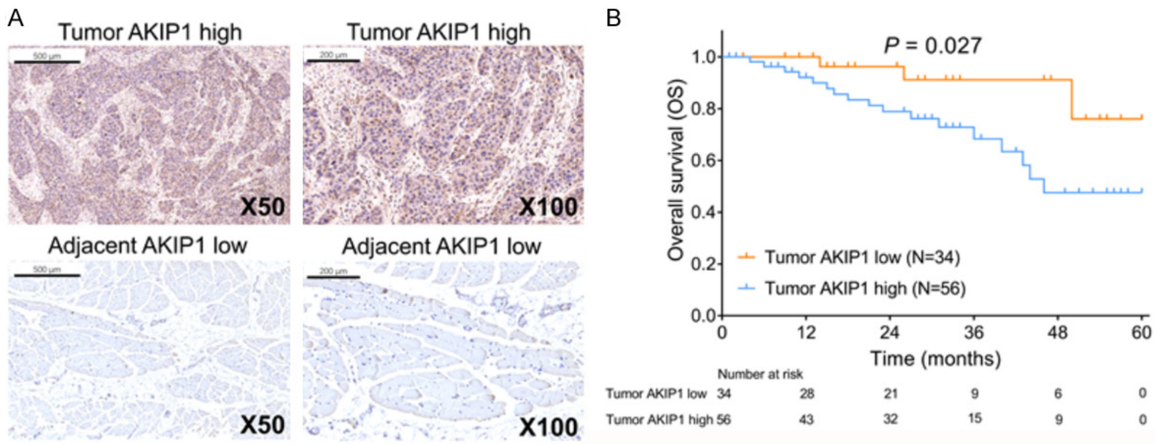

Figure 8. Correlation between AKIP1 expression and overall survival, OS. Examples of tumor or adjacent tissues with AKIP1 high/low expression (A); Correlation between AKIP1 expression and OS in TSCC patients (B).

Table 1. AKIP1 expression

Sample	AKIP1 low expression	AKIP1 high expression	*P* value
Tumor tissue	34 (37.8)	56 (62.2)	<0.001
Adjacent tissue	61 (67.8)	29 (32.2)	

revealed that AKIP1 knockdown inhibits cell growth by targeting Slug-induced epithelial-mesenchymal transition in gastric cancer [11]. In addition, AKIP1 expression enhances non-small-cell lung cancer cell viability and fibronectin and ZEB1 expression but represses apoptosis and E-cadherin expression [26]. Furthermore, AKIP1 downregulation suppresses breast cancer cell motility by inactivating the Akt/GSK-3β/Snail pathway [13]. Another recent study illustrated the ability of AKIP1 overexpression to enhance CC cell migration and invasion and facilitate epithelial-mesenchymal transition by activating NF-κB signaling through the PI3K/Akt/IKKβ pathway [12].

Given the carcinogenic role of AKIP1, we hypothesized that AKIP1 might function as a tumor promoter in TSCC. Relevant studies on this topic are limited. We discovered that AKIP1 expression was higher in human TSCC cell lines compared to NHOK cells. One possible reason could be that AKIP1 regulates various genes and pathways to enhance tumorigenesis in TSCC. In addition, we also examined the effect of AKIP1 on cellular functions in TSCC, and we discovered that AKIP1 promoted TSCC cell growth and metastasis. Probable reasons were as follows: (1) According to our subsequent experiments, AKIP1 regulates the mTOR, PI3K-Akt, MAPK, Hippo, and Wnt signaling pathways, and these 5 cancer-related pathways are involved in TSCC progression [21-25]. (2) AKIP1 targets multiple oncogenes (including NF-κB and ZEB1) to promote cell growth, migration, and invasion in TSCC [12, 26].

To explore the comprehensive molecular mechanism of AKIP1 and the relevant landscape in TSCC pathogenesis, we performed RNA sequencing and bioinformatic analyses after AKIP1 modification in TSCC cells. We found 436 accordant DEGs, including 240 DEGs upregulated in the AKIP1-OE group vs. NC-OE group and downregulated in the AKIP1-KD group vs. NC-KD group as well as 196 DEGs downregulated in the AKIP1-OE group vs. NC-OE group and upregulated in the AKIP1-KD group vs. NC-KD group. Then, some accordant DEGs were principally concentrated in the mTOR, PI3K-Akt, MAPK, Hippo, and Wnt signaling pathways. The following information regarding these pathways is important in this context: (1) The PI3K/Akt pathway served as a survival regulator during cellular stress [27]. Tumors persist in an intrinsically stressful environment; hence, the role of the PI3K/Akt pathway seems to be essential in cancer [28]; (2) mTOR is a protein kinase and important in the regulation of cell survival, metabolism, and growth in cancer [29, 30]; (3) MAPK signaling plays an essential role in cell viability and survival [31]; (4) Wnt signaling is tightly related to cancer, including colorectal cancer [32] and

Table 2. Relationship of tumor AKIP1 expression with clinical features

Item	Total patients (N=90)	Tumor AKIP1 expression		*P* value
		Low (N=34)	High (N=56)	
Age (years), mean ± SD	57.5±11.7	60.0±11.3	55.9±11.9	0.111
Gender, No. (%)				0.518
Male	67 (74.4)	24 (70.6)	43 (76.8)	
Female	23 (25.6)	10 (29.4)	13 (23.2)	
Pathologic grade, No. (%)				0.917
G1	14 (15.6)	6 (17.6)	8 (14.3)	
G2	64 (71.1)	23 (67.7)	41 (73.2)	
G3	12 (13.3)	5 (14.7)	7 (12.5)	
T stage, No. (%)				0.003
T1	15 (16.7)	12 (35.3)	3 (5.4)	
T2	48 (53.3)	15 (44.1)	33 (58.9)	
T3	27 (30.0)	7 (20.6)	20 (35.7)	
N stage, No. (%)				0.022
N0	56 (62.3)	26 (76.5)	30 (53.6)	
N1	30 (33.3)	8 (23.5)	22 (39.3)	
N2	4 (44.4)	0 (0.0)	4 (7.1)	
TNM stage, No. (%)				<0.001
Stage I	14 (15.6)	12 (35.3)	2 (3.6)	
Stage II	37 (41.1)	13 (38.2)	24 (42.9)	
Stage III	35 (38.9)	9 (26.5)	26 (46.4)	
Stage IV	4 (4.4)	0 (0.0)	4 (7.1)	
Adjuvant radiotherapy, No. (%)				0.053
No	24 (26.7)	13 (38.2)	11 (19.6)	
Yes	66 (73.3)	21 (61.8)	45 (80.4)	

Table 3. OS-related factors

Item	Univariate Cox regression		Multivariate Cox regression	
	hazard ratio (95% confidence interval)	*P* value	hazard ratio (95% confidence interval)	*P* value
Tumor AKIP1 high expression	3.649 (1.068-12.470)	0.039	3.118 (0.746-13.037)	0.119
Age >60 years	1.220 (0.502-2.964)	0.660	0.783 (0.284-2.156)	0.636
Gender (male)	1.789 (0.595-5.376)	0.300	1.680 (0.479-5.895)	0.418
Pathological grade (G3 vs. G1/2)	2.467 (0.947-6.428)	0.065	2.877 (1.008-8.210)	0.048
TNM stage (III/IV vs. II/I)	9.728 (2.837-33.356)	<0.001	9.982 (2.560-38.927)	0.001
Adjuvant radiotherapy	1.031 (0.409-2.600)	0.948	0.419 (0.147-1.198)	0.104

prostate cancer [33]; (5) the Hippo signaling pathway is a highly conserved pathway that is important in organ growth, cell differentiation and stem cell self-renewal [34, 35]. To further validate these 5 cancer-related pathways, we also performed RT-qPCR and found that AKIP1 overexpression activated these 5 cancer-related pathways, whereas AKIP1 knockdown inactivated these 5 cancer-related pathways. Taken together, our findings indicated that AKIP1 regulated multiple cancer-related pathways in TSCC, providing novel evidence for the molecular mechanisms by which AKIP1 regulates TSCC tumorigenesis and progression. However, the detailed mechanism by which AKIP1 regulates these 5 cancer-related pathways in TSCC remains unknown. Hence, further study is essential.

In addition to the biologic role of AKIP1 in several cancers, its clinical implication has also been illustrated in cancer patients. For instance, in gastric cancer patients, AKIP1 expression is upregulated in gastric cancer specimens, and its overexpression is obviously related to larger tumor size, elevated TNM stage, worse lymph node metastasis, and poor OS [11]. In NSCLC patients, AKIP1 is related to larger tumor size, worse lymph node metastasis, and higher TNM stage [26]. In addition, AKIP1 overexpression is positively associated with alpha-fetoprotein and carbohydrate antigen levels; more importantly, AKIP1 is related to shorter OS [9]. Although the clinical implication of AKIP1 has been explored in several types of cancer, its role in TSCC patients remains unknown. In this study, the data showed that AKIP1 expression was higher in tumor tissue compared with adjacent tissue, and high tumor expression was correlated with enhanced T, N and TNM stage. These findings may be due to the fact that AKIP1 regulates several carcinogenic genes (such as NF-κB [12] and ZEB1 [26]) as well as cancer-related pathways (such as mTOR, PI3K-Akt, MAPK, Hippo, and Wnt signaling pathways, abovementioned) to promote tumor progression, which is related to worse clinicopathologic features in TSCC patients. In addition, we also found that high tumor expression was related to shorter OS in TSCC patients. One possible reason was that AKIP1 was related to worse clinicopathologic features (mentioned above), eventually causing shorter OS in TSCC patients. Another possible explanation was that AKIP1 might regulate multiple pathways (such as Slug-induced EMT [11] and PI3K/Akt/IKKβ [12]) to increase drug resistance, subsequently decreasing treatment outcomes and leading to shorter OS in TSCC patients.

In conclusion, AKIP1 promotes cell proliferation, migration, and invasion and activates a variety of cancer-related pathways (e.g., mTOR, PI3K-Akt, MAPK, Hippo, and Wnt signaling pathways) in TSCC cells. AKIP1 is also related to advanced tumor stages and worse survival in TSCC patients. These findings indicate that AKIP1 might be a I therapeutic target that regulates multiple cancer-related pathways in TSCC.

Disclosure of conflict of interest

None.

Address correspondence to: Shijun Zhang, Department of Orthopaedics, Qilu Hospital of Shandong University, No. 107 Wenhuaxi Road, Lixia District, Jinan 250012, Shandong, China. Tel: +86-0531-82166533; E-mail: shijiuji12550@163.com

References

[1] Bray F, Ferlay J, Soerjomataram I, Siegel RL, Torre LA and Jemal A. Global cancer statistics 2018: GLOBOCAN estimates of incidence and mortality worldwide for 36 cancers in 185 countries. CA Cancer J Clin 2018; 68: 394-424.

[2] Yu X and Li Z. MicroRNA expression and its implications for diagnosis and therapy of tongue squamous cell carcinoma. J Cell Mol Med 2016; 20: 10-16.

[3] Almangush A, Heikkinen I, Makitie AA, Coletta RD, Laara E, Leivo I and Salo T. Prognostic biomarkers for oral tongue squamous cell carcinoma: a systematic review and meta-analysis. Br J Cancer 2017; 117: 856-866.

[4] Chen J, Liu L, Cai X, Yao Z and Huang J. Progress in the study of long noncoding RNA in tongue squamous cell carcinoma. Oral Surg Oral Med Oral Pathol Oral Radiol 2020; 129: 51-58.

[5] Hussein AA, Forouzanfar T, Bloemena E, de Visscher J, Brakenhoff RH, Leemans CR and Helder MN. A review of the most promising biomarkers for early diagnosis and prognosis prediction of tongue squamous cell carcinoma. Br J Cancer 2018; 119: 724-736.

[6] Gore SM, Crombie AK, Batstone MD and Clark JR. Concurrent chemoradiotherapy compared with surgery and adjuvant radiotherapy for oral cavity squamous cell carcinoma. Head Neck 2015; 37: 518-523.

[7] Iyer NG, Tan DS, Tan VK, Wang W, Hwang J, Tan NC, Sivanandan R, Tan HK, Lim WT, Ang MK, Wee J, Soo KC and Tan EH. Randomized trial comparing surgery and adjuvant radiotherapy versus concurrent chemoradiotherapy in patients with advanced, nonmetastatic squamous cell carcinoma of the head and neck: 10-year update and subset analysis. Cancer 2015; 121: 1599-1607.

[8] P Oc, Pillai G, Patel S, Fisher C, Archer D, Eccles S and Rhys-Evans P. Tumour thickness predicts cervical nodal metastases and survival in early oral tongue cancer. Oral Oncol 2003; 39: 386-390.

[9] Fang T and Lu Q. A-kinase interacting protein 1 (AKIP1) associates with advanced overall disease condition, tumor properties, and unfavorable prognosis in hepatocellular carcinoma patients. J Clin Lab Anal 2020; 34: e23213.

[10] Jiang W, Yang W, Yuan L and Liu F. Upregulation of AKIP1 contributes to metastasis and progression and predicts poor prognosis of patients with colorectal cancer. Onco Targets Ther 2018; 11: 6795-6801.

[11] Chen D, Cao G and Liu Q. A-kinase-interacting protein 1 facilitates growth and metastasis of gastric cancer cells via Slug-induced epithelial-mesenchymal transition. J Cell Mol Med 2019; 23: 4434-4442.
[12] Zhang X, Liu S and Zhu Y. A-kinase-interacting protein 1 promotes EMT and metastasis via PI3K/Akt/IKKbeta pathway in cervical cancer. Cell Biochem Funct 2020; 38: 782-791.
[13] Mo D, Li X, Li C, Liang J, Zeng T, Su N, Jiang Q and Huang J. Overexpression of AKIP1 predicts poor prognosis of patients with breast carcinoma and promotes cancer metastasis through Akt/GSK-3beta/Snail pathway. Am J Transl Res 2016; 8: 4951-4959.
[14] Lin R, Zhao S, Su L, Chen X, Xu C, He Q, Zhuo C and Ye Y. A kinase-interacting protein 1 may serve as a potential biomarker for deteriorative tumor features and poor prognosis in gastric cancer patients. J Clin Lab Anal 2020; 34: e23350.
[15] Li Y, Wan Q, Wang W, Mai L, Sha L, Mashrah M, Lin Z and Pan C. LncRNA ADAMTS9-AS2 promotes tongue squamous cell carcinoma proliferation, migration and EMT via the miR-600/EZH2 axis. Biomed Pharmacother 2019; 112: 108719.
[16] Sun J, Lu Z, Deng Y, Wang W, He Q, Yan W and Wang A. Up-regulation of INSR/IGF1R by C-myc promotes TSCC tumorigenesis and metastasis through the NF-kappaB pathway. Biochim Biophys Acta Mol Basis Dis 2018; 1864: 1873-1882.
[17] Head SR, Komori HK, LaMere SA, Whisenant T, Van Nieuwerburgh F, Salomon DR and Ordoukhanian P. Library construction for next-generation sequencing: overviews and challenges. Biotechniques 2014; 56: 61-64, 66, 68, passim.
[18] Trapnell C, Pachter L and Salzberg SL. TopHat: discovering splice junctions with RNA-Seq. Bioinformatics 2009; 25: 1105-1111.
[19] Love MI, Huber W and Anders S. Moderated estimation of fold change and dispersion for RNA-seq data with DESeq2. Genome Biol 2014; 15: 550.
[20] Huang DW, Sherman BT, Tan Q, Kir J, Liu D, Bryant D, Guo Y, Stephens R, Baseler MW, Lane HC and Lempicki RA. DAVID bioinformatics resources: expanded annotation database and novel algorithms to better extract biology from large gene lists. Nucleic Acids Res 2007; 35: W169-175.
[21] Lin Z, Sun L, Xie S, Zhang S, Fan S, Li Q, Chen W, Pan G, Wang W, Weng B, Zhang Z, Liu B and Li J. Chemotherapy-induced long non-coding RNA 1 promotes metastasis and chemo-resistance of TSCC via the Wnt/beta-catenin signaling pathway. Mol Ther 2018; 26: 1494-1508.
[22] Wang ZY, Hu M, Dai MH, Xiong J, Zhang S, Wu HJ, Zhang SS and Gong ZJ. Upregulation of the long non-coding RNA AFAP1-AS1 affects the proliferation, invasion and survival of tongue squamous cell carcinoma via the Wnt/beta-catenin signaling pathway. Mol Cancer 2018; 17: 3.
[23] Pan ST, Qin Y, Zhou ZW, He ZX, Zhang X, Yang T, Yang YX, Wang D, Qiu JX and Zhou SF. Plumbagin induces G2/M arrest, apoptosis, and autophagy via p38 MAPK- and PI3K/Akt/mTOR-mediated pathways in human tongue squamous cell carcinoma cells. Drug Des Devel Ther 2015; 9: 1601-1626.
[24] Xue D, Pan ST, Zhou X, Ye F, Zhou Q, Shi F, He F, Yu H and Qiu J. Plumbagin enhances the anticancer efficacy of cisplatin by increasing intracellular ROS in human tongue squamous cell carcinoma. Oxid Med Cell Longev 2020; 2020: 5649174.
[25] Gu Y, Liu H, Kong F, Ye J, Jia X, Zhang Z, Li N, Yin J, Zheng G and He Z. miR-22/KAT6B axis is a chemotherapeutic determiner via regulation of PI3k-Akt-NF-kB pathway in tongue squamous cell carcinoma. J Exp Clin Cancer Res 2018; 37: 164.
[26] Chen H, Yan S, Dong L and Li X. A-kinase-interacting protein 1 overexpression correlates with deteriorative tumor features and worse survival profiles, and promotes cell proliferation but represses apoptosis in non-small-cell lung cancer. J Clin Lab Anal 2020; 34: e23061.
[27] Datta SR, Brunet A and Greenberg ME. Cellular survival: a play in three Akts. Genes Dev 1999; 13: 2905-2927.
[28] Porta C, Paglino C and Mosca A. Targeting PI3K/Akt/mTOR signaling in cancer. Front Oncol 2014; 4: 64.
[29] Hua H, Kong Q, Zhang H, Wang J, Luo T and Jiang Y. Targeting mTOR for cancer therapy. J Hematol Oncol 2019; 12: 71.
[30] Tian T, Li X and Zhang J. mTOR signaling in cancer and mTOR inhibitors in solid tumor targeting therapy. Int J Mol Sci 2019; 20: 755.
[31] Low HB and Zhang Y. Regulatory roles of MAPK phosphatases in cancer. Immune Netw 2016; 16: 85-98.
[32] Zhan T, Rindtorff N and Boutros M. Wnt signaling in cancer. Oncogene 2017; 36: 1461-1473.
[33] Murillo-Garzon V and Kypta R. WNT signalling in prostate cancer. Nat Rev Urol 2017; 14: 683-696.
[34] Park JH, Shin JE and Park HW. The role of Hippo pathway in cancer stem cell biology. Mol Cells 2018; 41: 83-92.
[35] Harvey KF, Zhang X and Thomas DM. The Hippo pathway and human cancer. Nat Rev Cancer 2013; 13: 246-257.

Supplementary Table 1. Primers

Gene	Forward Primer (5'-3')	Reverse Primer (5'-3')
AKIP1	AGAACATCTCTAAGGACCTCTACAT	TCCAGAATCAACTGCTACCACAT
Akt	GTTCTCTGAGGACCGCACAC	TCCAGCATTAGATTCTCCAACTTGA
RRAGB	CAGTGTAAAGAGCAGCGTGATG	AAGCAGCGAAGTTAGAGTTCCT
SLC38A9	TTCCTGCTGTTCCAGATGATGAC	TCCACATGCTGCTCCTGAATATC
EIF4B	AGAACGGCTACAGAAGGAACAAG	TTAGAAGTTGGAGAGTGGCAATCTT
IKBKB	CAAGGTCCGTGGTCCTGTCA	TGCTCTTCTTCTTCCGTCTGTAAC
LRP6	GCTTCTGTGCCTCTTGGTTATGT	TGGTGCTTGAAGAACTACTTGATGA
ATP6V1D	AGGTGACTTCAGCACTACAGTTATC	CACGCCTGTTGGTTATCTTAATAGC
PIK3CA	CGAAGTATGTTGCTATCCTCTGAAC	CGTCTGGAATAAGATGGCATTGTAA
MIOS	CAACCGAACAATGTCAGACTTCAC	CTCCACACCTGCTCTGTATCAAG
PRKAA1	GACAGAAGATTCGGAGCCTTGAT	TCATCCAGCCTTCCATTCTTACAG
PRKAA2	TTCTGTCGCCACTCTCCTGAT	GCTTGGTTCATTATTCTCCGATTGT
FNIP2	GCACTGACCACACGGAACTC	CTGCTGCTACTGCTGCTGAC
RPS6KA2	CGAGACCTGAAGCCGAGTAAC	TCACACGCCGCATCATAGC
RPS6KA3	GAGACTGACTGCTGCTCTTGTG	AACTGGTGACTGATTACGGTTCAA
RRAGC	CATTCCACAACTGCCGACCTT	GCACTTCCACTTCCATCTTCCTT
BRAF	GCATGGTGATGTGGCAGTGA	TGGATGATTGACTTGGCGTGTAA
STK11	GACATCATCTACACTCAGGACTTCA	CGCCTCTGTGCCGTTCATAC
WNT2	TCTCGGTGGAATCTGGCTCTG	CCTGGCACATTATCGCACATCA
WNT3	GTAGTAGAGAAGCACCGTGAGTC	CAGAGCAGATCGCAGCCATC
WNT5A	CTTGGTGGTCGCTAGGTATGAATA	GATGTCGGAATTGATACTGGCATT
WNT9A	ACTGCCTTCCTCTATGCCATCT	CCTTGACGAACTTGCTGCTGTA
FZD3	CAGTTACAGAGGAATGGAGGAGAG	CTGATGCTGCTATGTCGTGACT
SLC7A5	GTGTGATGACGCTGCTCTACG	CCGCTGAGGATGATGGTGAAG
FZD1	GCCATCAAGACCATCACCATCC	GCACGCTGAAGACGCCAAT
FZD7	CCTCTGTTCGTCTACCTCTTCATAG	GTCTTGGTGCCGTCGTGTT
FZD8	CCAATCAGTTCAACCACGACAC	AGCGGCTTCTTGTAGTCCTCTA
FNIP1	AGCCAGAGACGAGTGACAGATAA	GGAGAGTGAGTGCTTGCTACAG
TTI1	ACTGGAAGGTGAGACTGGAACT	CGAGGAAGAGATGTGGCAAGG
BCL2L11	ACCTTCTGATGTAAGTTCTGAGTGT	GCTTGTGGCTCTGTCTGTAGG
CDK6	GCTTCTCCGAGGTCTGGACTT	CCACTGAGGTTAGAGCCATCTG
CREB3	CTCCTTCTGCCTCCTCCTTGT	ACACAGTCTGAGCCGTCCAA
CDC37	AGGAGAAGGAGGAACTGGACAG	GCTCTTGCTGAAGCCGTCTT
EGFR	GGACAGCATAGACGACACCTTC	CCTGGCTTGGACACTGGAGA
FGFR4	GCCGACACAAGAACATCATCAAC	GTCCTCAGTCACCAGCACATTG
FLT1	AACCTCACTGCCACTCTAATTGTC	AGTCACACCTTGCTTCGGAATG
GNB1	ATCACCTCTGTCTCCTTCTCCAA	AGCCATGCCATCGTCAGTCA
PKN3	CAATGCCTGTCACCAACTGTC	AAGATGCGTTCCTGCCTCTG
HGF	CGCTGACAATACTATGAATGACACT	ATGCTCGTGAGGATACTGAGAATC
HSP90AA1	ATCCACCACTCTACTCTGTCTCTG	CTCAACCTCCTCCTCCTCCATC
HSP90AB1	GAATCCACGAAGACTCCACTAACC	TTCCGCACTCGCTCCACAA
ITGA1	AGCCTATGATTGGAATGGAACAGT	CCAGAAGAAGCAGTAGCAGAGTT
ITGA7	GCCACTCTGCCTGTCCAATG	GGAGGTGCTAAGGATGAGGTAGA
ITGB3	ATGAGGAAGTGAAGAAGCAGAGTG	GTAGTGGAGGCAGAGTAATGATTGT
ITGB4	GCTCTACACGGACACCATCTG	CCACCATCTTGACCTTGAAGTTG
MYC	GAGGAGGAACAAGAAGATGAGGAAG	GCTGCGTAGTTGTGCTGATGT
NFKB1	TCATCCACCTTCATTCTCAACTTGT	CTCCACCACATCTTCCTGCTTAG

PDGFA	CGTCCGCCAACTTCCTGAT	AATGCTCCTCTAACCTCACCTG
PPP2R5B	CTGTGCTGCCTGCTGTGTT	TCCTCCAGACCTTGCCATAACT
PRLR	TCCAGCGACCTTCATTCAGATAC	TCCACCAGCAAGTCCTCATAGT
BCL2L1	GGACTGAATCGGAGATGGAGAC	TCGGCTGCTGCATTGTTCC
TLR2	ACATTAGCAACAGTGACCTACAGAG	GGCTTGAACCAGGAAGACGATAA
HSP90B1	TTAGGTTCCAGTCTTCTCATCATCC	TTCACTCCTTCCTTGGCAACATT
VEGFB	TGGTGGTGCCCTTGACTGT	CATTCACACTGGCTGTGTTCTTC
VWF	CTTGGTCACATCTTCACATTCACTC	TCATTGGCTCCGTTCTCATCAC
YWHAB	GGAATGAGAAGAAGCAGCAGATG	TTGTTGTCTCCAGATGCCACTT
FGF18	TCCTGCTGCTGTGCTTCCA	TTCCGTCTCCTTGCCCTTGAT
CCNE1	ACTATTGTGTCCTGGCTGAATGTAT	GTTCTCTATGTCGCACCACTGAT
LPAR2	CCAGTGCTACTACAACGAGACC	GAGGCGATGGCTGCTATGAC
TAB2	GATGCCTGCTGTGCTGTTCT	TAATGCTGTGCGTTAGAGTCCTAC
FLNB	ACTGCCACCTTCACCATCGT	ACCGCCTGCTGTCATCTGT
MAPK8IP2	TCCACCTTCCACTCGCTGTC	CTCATCGTCCTCCTCTTCATTGTC
GNA12	TGAAGACCGTGAGCATCAAGAAG	GTGGTGAAGTGGTGGAAGAGTG
HSPA2	ACGCAGACCTTCACCACCTA	GTCAATGTCGTCCTTGCTCAGA
HSPA6	CACCACCTACTCGGACAACCA	GTCACGCTCAGGATGCCATTAG
HSPA8	ATGATATTGTCCTGGTTGGTGGTT	GAATGGTGGTATTACGCTTGATGAG
FAS	GAAGGACATGGCTTAGAAGTGGAA	CTTGGTGTTGCTGGTGAGTGT
ARRB2	GTAGATGGCGTGGTGCTTGTG	AGGTGGCGATGAACAGGTCTT
MAX	CGTAGGGACCACATCAAAGACAG	CGATGAAGGACAGGAGTACACAAT
NFATC1	CAGCGGAGGAAGAACACTATGG	CGGTGTGGAGGTCTGAAGGT
PAK1	TTGAATGTGAAGGCTGTGTCTGA	GCATCTGGTGGAGTGGTGTTAT
PPP3CC	AGGAAGGACGACTGGAAGAGG	ACATACTGTGATTGGAGCATCTACT
RAC2	CGTCTTCCTCATCTGCTTCTCC	TTCACCGAGTCAATCTCCTTGG
RAP1A	CTTGGTTCAGGAGGCGTTGG	GAGCATACACTGTTGGCAATCG
BDNF	GCTTGACATCATTGGCTGACACT	GGCACTTGACTACTGAGCATCAC
TRAF2	AGCAGAAGGTCTTGGAGATGGA	CGTCGCCGTTCAGGTAGATAC
DUSP16	GGAGCGTGGAGGACAATTACC	AGGCAGAGTAGAAGTGTGAGGA
PLCB3	CCATTGCCGAGACTGCCTTC	GGTGCCGCTTCTTGTTCTTCA
DLG1	CCAACTCTTCTTCTCAGCCTGTT	TCCTTCTCCATCTTCTCCTCCTAC
GLI2	TCAGAGCCATCAAGACCGAGAG	TCCACGCCACTGTCATTGTTG
TGFB2	AGTGCCTGAACAACGGATTGAG	GCCATTCGCCTTCTGCTCTT
TGFBR2	GAGGAGCGGAAGACGGAGTT	ACACAGGCAGCAGGTTAGGT
PARD6A	GCCATAACCTCATTGTCACTGTCA	GTCACTGCTGTCATCGTCACTATC
GAPDH	GACCACAGTCCATGCCATCAC	ACGCCTGCTTCACCACCTT

Supplementary Table 2. Top 50 DEGs in accordance with RNA-seq

Gene ID	Symbol	OE log_2FC	OE *P* value	OE P_{adj} value	KD log_2FC	KD *P* value	KD P_{adj} value	OE Trend	KD Trend	Mean Absolute log_2FC
ENSG00000078487	ZCWPW1	-5.04470429	4.8529E-06	8.03546E-05	5.940813456	7.33362E-08	1.04834E-06	DOWN	UP	5.492758873
ENSG00000189180	ZNF33A	-5.493646254	3.1345E-16	2.95798E-14	3.666698434	3.09598E-13	9.76324E-12	DOWN	UP	4.580172344
ENSG00000130592	LSP1	3.651742216	4.13856E-05	0.000530032	-4.868205163	3.90845E-08	5.86782E-07	UP	DOWN	4.25997369
ENSG00000125375	ATP5S	-5.412466177	4.27361E-06	7.19009E-05	2.807036409	0.000197644	0.001404493	DOWN	UP	4.109751293
ENSG00000157764	BRAF	2.65362302	5.65461E-06	9.26515E-05	-5.525251942	8.17137E-21	6.65967E-19	UP	DOWN	4.089437481
ENSG00000177283	FZD8	3.652998409	1.4606E-05	0.000213909	-4.078323911	1.14429E-06	1.33352E-05	UP	DOWN	3.86566116
ENSG00000164654	MIOS	2.68652491	8.21204E-05	0.000951331	-4.962812136	1.67177E-13	5.40784E-12	UP	DOWN	3.824668523
ENSG00000138678	GPAT3	2.746918495	0.000401989	0.003666692	-4.732803023	3.27766E-07	4.23229E-06	UP	DOWN	3.739860759
ENSG00000114859	CLCN2	2.9526165	6.25369E-08	1.53776E-06	-4.452991876	5.39649E-17	2.82214E-15	UP	DOWN	3.702804188
ENSG00000131844	MCCC2	2.841166282	8.52607E-12	4.1477E-10	-4.56356982	1.44153E-17	7.97035E-16	UP	DOWN	3.702368051
ENSG00000148082	SHC3	2.829805212	5.16332E-05	0.000640363	-4.570074323	2.95279E-11	7.23837E-10	UP	DOWN	3.699939767
ENSG00000058729	RIOK2	-3.224433518	2.232E-05	0.000312306	4.099805223	6.10595E-08	8.94233E-07	DOWN	UP	3.66211937
ENSG00000107829	FBXW4	2.894902453	8.07298E-07	1.58319E-05	-4.415918702	1.57154E-14	5.80129E-13	UP	DOWN	3.655410578
ENSG00000169629	RGPD8	-4.607986898	5.2828E-11	2.26295E-09	2.644300229	1.4096E-06	1.61717E-05	DOWN	UP	3.626143563
ENSG00000185090	MANEAL	-4.0933625	1.36698E-10	5.58858E-09	3.139636858	1.32781E-12	3.86666E-11	DOWN	UP	3.616499679
ENSG00000037757	MRI1	-5.236041216	3.20103E-22	5.58003E-20	1.993924104	2.03827E-08	3.2058E-07	DOWN	UP	3.61498266
ENSG00000180304	OAZ2	3.100498675	4.46152E-06	7.46303E-05	-4.115288328	7.86385E-10	1.57164E-08	UP	DOWN	3.607893502
ENSG00000081803	CADPS2	-3.482711572	3.13659E-11	1.40597E-09	3.73200361	6.0791E-11	1.40773E-09	DOWN	UP	3.607357591
ENSG00000099795	NDUFB7	-4.621937325	1.19498E-11	5.72452E-10	2.550258406	7.19216E-08	1.03047E-06	DOWN	UP	3.586097866
ENSG00000174744	BRMS1	3.868741333	5.22567E-09	1.5542E-07	-3.285423063	5.96192E-09	1.02645E-07	UP	DOWN	3.577082198
ENSG00000174840	PDE12	-3.032498674	0.001876908	0.013339228	4.11497239	1.97276E-05	0.000179161	DOWN	UP	3.573735532
ENSG00000117586	TNFSF4	-5.191751194	1.63199E-12	8.9057E-11	1.858923794	0.005698753	0.024869625	DOWN	UP	3.525337494
ENSG00000246922	UBAP1L	-3.087593561	0.0001284	0.001397699	3.931878463	4.77914E-09	8.37751E-08	DOWN	UP	3.509736012
ENSG00000101407	TTI1	-4.840843637	4.37287E-09	1.3225E-07	2.152893295	8.42461E-07	1.00991E-05	DOWN	UP	3.496868466
ENSG00000108960	MMD	3.420254146	1.49274E-06	2.79633E-05	-3.562402182	2.73728E-07	3.56017E-06	UP	DOWN	3.491328164
ENSG00000146802	TMEM168	-3.094436186	0.005662937	0.032633388	3.821423352	0.000476423	0.003024574	DOWN	UP	3.457929769
ENSG00000160408	ST6GALNAC6	1.190282459	0.003399007	0.0217104	-5.657406093	7.04595E-06	7.05776E-05	UP	DOWN	3.423844276
ENSG00000204172	AGAP9	2.462940185	0.000261475	0.002545983	-4.271878572	1.59526E-10	3.48211E-09	UP	DOWN	3.367409378
ENSG00000163517	HDAC11	-5.083905873	1.98156E-07	4.34801E-06	1.622801671	0.008108658	0.03313962	DOWN	UP	3.353353772
ENSG00000057657	PRDM1	-3.862088182	3.89365E-10	1.40026E-08	2.766003625	2.61857E-06	2.87538E-05	DOWN	UP	3.314045904
ENSG00000137502	RAB30	-3.181342858	1.22751E-07	2.81139E-06	3.294611099	1.60396E-09	3.0688E-08	DOWN	UP	3.237976978
ENSG00000006125	AP2B1	2.464479536	9.33556E-08	2.20246E-06	-4.007400919	1.07723E-19	7.55322E-18	UP	DOWN	3.235940228
ENSG00000063046	EIF4B	2.727432594	0.000248876	0.002440342	-3.74364279	1.81185E-07	2.43214E-06	UP	DOWN	3.235537692
ENSG00000145375	SPATA5	-4.376289562	1.02063E-13	6.67185E-12	2.044420815	0.00044054	0.002829691	DOWN	UP	3.210355188
ENSG00000085831	TTC39A	-3.327767887	8.40334E-06	0.000133846	3.042365006	5.01674E-06	5.20373E-05	DOWN	UP	3.185066446
ENSG00000165923	AGBL2	-4.612988013	1.16859E-14	8.42932E-13	1.732241182	0.000300251	0.002024959	DOWN	UP	3.172614597

ENSG00000121236	TRIM6	2.990440687	2.77824E-10	1.03779E-08	-3.343093998	2.80793E-13	8.92212E-12	UP	DOWN	3.166767342
ENSG00000172748	ZNF596	-3.154456138	6.35377E-15	4.92261E-13	3.135138951	1.67479E-18	1.05102E-16	DOWN	UP	3.144797545
ENSG00000113971	NPHP3	2.217479054	0.005543974	0.032095212	-4.068972569	1.6293E-07	2.20836E-06	UP	DOWN	3.143225811
ENSG00000019991	HGF	2.795801684	2.42151E-10	9.18197E-09	-3.453426526	9.22378E-20	6.54055E-18	UP	DOWN	3.124614105
ENSG00000106538	RARRES2	2.368913084	2.01201E-06	3.68116E-05	-3.815587565	1.29086E-17	7.20072E-16	UP	DOWN	3.092250325
ENSG00000171302	CANT1	-2.70932436	3.39667E-08	8.83854E-07	3.431973094	1.14004E-14	4.28403E-13	DOWN	UP	3.070648727
ENSG00000042317	SPATA7	2.830600498	5.72066E-12	2.88353E-10	-3.285239074	5.83917E-20	4.23627E-18	UP	DOWN	3.057919786
ENSG00000107175	CREB3	2.551271756	3.16733E-10	1.16921E-08	-3.547484569	6.36788E-20	4.59329E-18	UP	DOWN	3.049378162
ENSG00000158296	SLC13A3	2.387282866	0.000120714	0.001336053	-3.676658958	1.61502E-09	3.08525E-08	UP	DOWN	3.031970912
ENSG00000156427	FGF18	2.852787484	2.20442E-11	1.00245E-09	-3.210093648	5.00182E-18	2.97526E-16	UP	DOWN	3.031440566
ENSG00000196152	ZNF79	2.62159661	5.14684E-07	1.05552E-05	-3.441247418	1.95549E-14	7.13468E-13	UP	DOWN	3.031422014
ENSG00000104524	PYCRL	2.480261992	2.9485E-05	0.00039749	-3.568172639	5.04018E-10	1.03365E-08	UP	DOWN	3.024217316
ENSG00000157240	FZD1	2.430275227	0.000135158	0.001457449	-3.594338701	7.42912E-09	1.25834E-07	UP	DOWN	3.012306964
ENSG00000133048	CHI3L1	2.091801855	0.003545805	0.022363517	-3.911247426	1.56398E-08	2.50696E-07	UP	DOWN	3.00152464

Top 50 DEGs were selected by the rank of mean absolute value of Log_2FC, which was calculated by the average of OE absolute log_2FC and KD absolute log_2FC.

Supplementary Table 3. Screened pathways*

Pathways#	Num of symbols	Proportion of symbols	Symbols	Fold enrichment	*P* value
mTOR signaling pathway	28	0.142	AKT3, RRAGB, SLC38A9, EIF4B, IKBKB, LRP6, ATP6V1D, PIK3CA, MIOS, PRKAA1, PRKAA2, FNIP2, RPS6KA2, RPS6KA3, RRAGC, BRAF, STK11, WNT2, WNT3, WNT5A, WNT9A, FZD3, SLC7A5, FZD1, FZD7, FZD8, FNIP1, TTI1	6.571	4.860E-15
PI3K-Akt signaling pathway	37	0.188	AKT3, BCL2L11, CDK6, CREB3, CDC37, EGFR, EIF4B, FGFR4, FLT1, GNB1, PKN3, HGF, HSP90AA1, HSP90AB1, IKBKB, ITGA1, ITGA7, ITGB3, ITGB4, MYC, NFKB1, PDGFA, PIK3CA, PPP2R5B, PRKAA1, PRKAA2, PRLR, BCL2L1, STK11, TLR2, HSP90B1, VEGFB, VWF, YWHAB, FGF18, CCNE1, LPAR2	3.884	1.759E-12
MAPK signaling pathway	31	0.157	AKT3, EGFR, FGFR4, TAB2, FLNB, MAPK8IP2, GNA12, HSPA2, HSPA6, HSPA8, FAS, IKBKB, ARRB2, MAX, MYC, NFATC1, NFKB1, PAK1, PDGFA, PPP3CC, RAC2, RAP1A, RPS6KA2, RPS6KA3, BDNF, BRAF, TGFB2, TGFBR2, TRAF2, DUSP16, FGF18	4.364	9.242E-12
Hippo signaling pathway	15	0.076	DLG1, GLI2, MYC, PARD6A, TGFB2, TGFBR2, WNT2, WNT3, WNT5A, WNT9A, YWHAB, FZD3, FZD1, FZD7, FZD8	3.497	8.037E-05
Wnt signaling pathway	14	0.071	LRP6, MYC, NFATC1, PLCB3, PPP3CC, RAC2, WNT2, WNT3, WNT5A, WNT9A, FZD3, FZD1, FZD7, FZD8	3.515	1.443E-04

*These pathways were screened out based on: (1) KEGG enrichment in accordance DEG, (2) correlation with TSCC malignancy and progression, which was confirmed by published studies. Based on *P* values, #pathways displayed in this table were ranked.

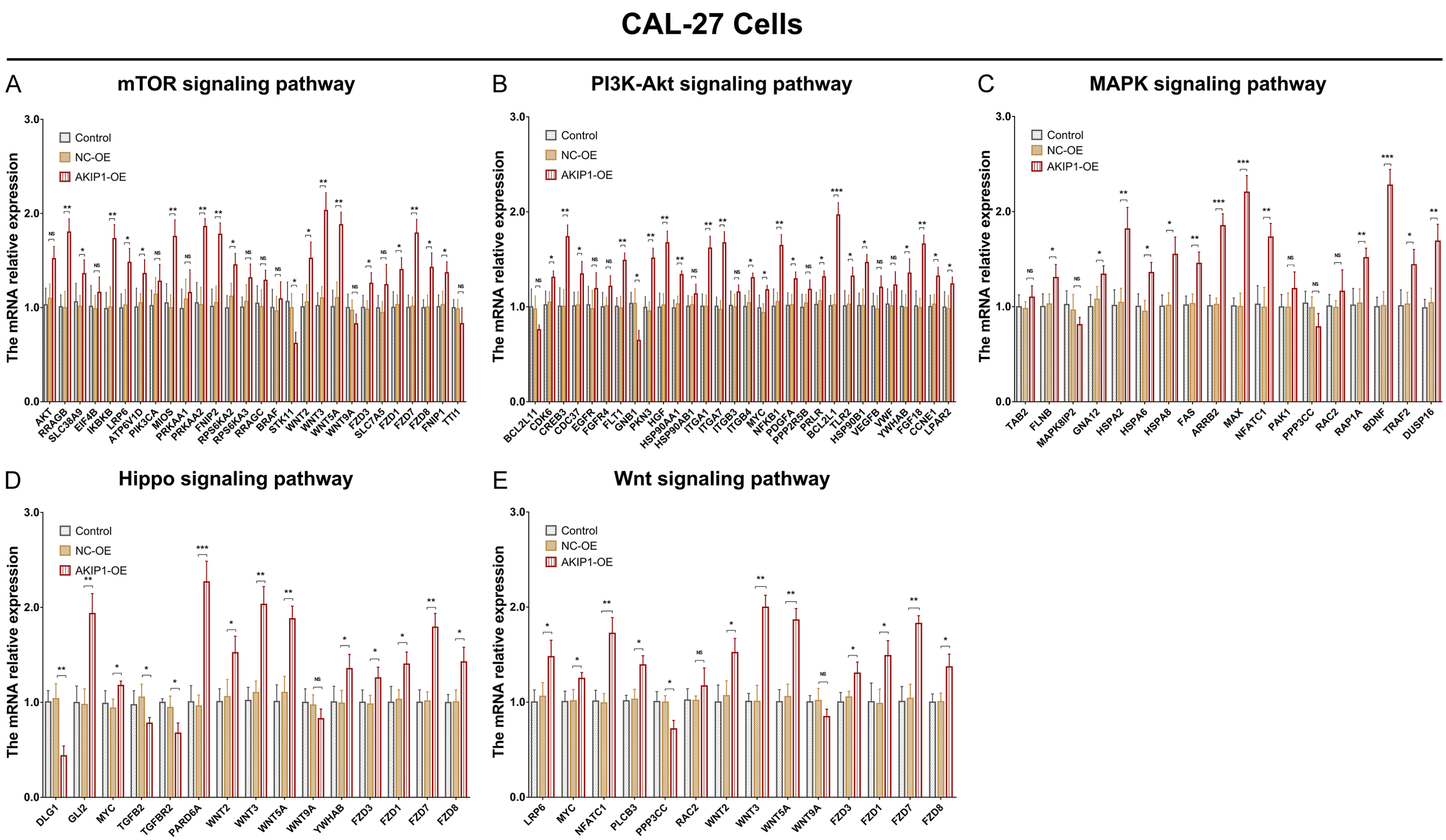
CAL-27 Cells
A
mTOR signaling pathway
B
PI3K-Akt signaling pathway
C
MAPK signaling pathway
D
Hippo signaling pathway
E
Wnt signaling pathway
Control
NC-OE
AKIP1-OE
The mRNA relative expression

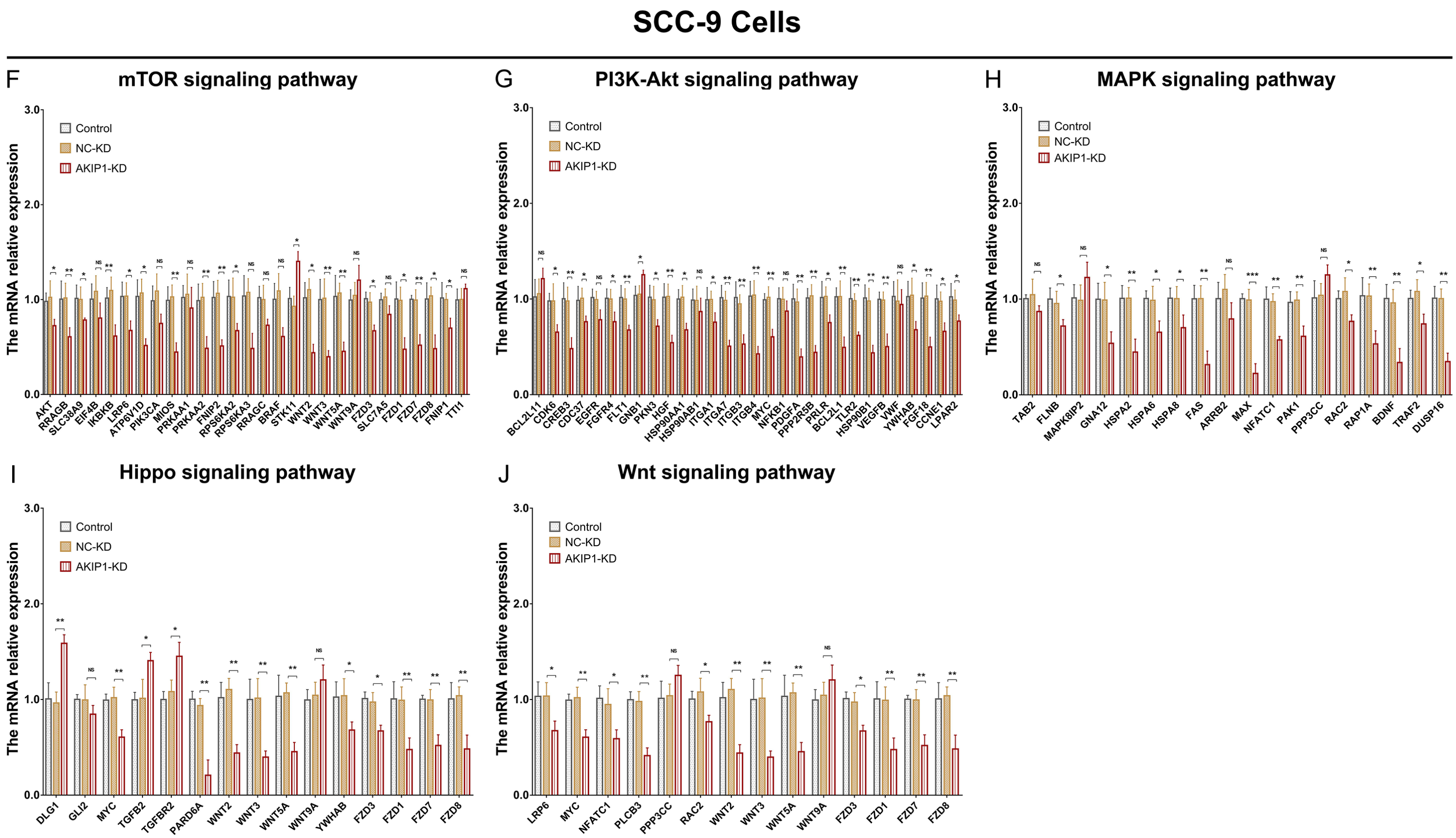

Supplementary Figure 1. Validation of 5 screened cancer-related pathways. Relative expression of DEGs implicated in the mTOR pathway, PI3K-Akt pathway, MAPK pathway, Hippo pathway, and Wnt pathway in the AKIP1-OE group vs. NC-OE group of CAL-27 cells (A-E) and the AKIP1-KD group vs. NC-KD group of SCC-9 cells (F-J).